International Journal of Research in Engineering, Science and Management
Volume-3, Issue-1, January-2020
www.ijresm.com | ISSN (Online): 2581-5792

Design and Analysis of Vortex Tube for Refrigeration using Computational Fluid Dynamics

R. Pavithra[1], M. Sekar[2]
[1]*PG Scholar, Department of Mechanical Engineering, Government College of Technology, Coimbatore, India*
[2]*Professor, Department of Mechanical Engineering, Government College of Technology, Coimbatore, India*

***Abstract*: Vortex tubes hold promise for developing low cost refrigeration and air conditioning systems. They do not require the use of any moving parts. They also do not consume energy when compressed air is available. In this study, a CFD is conducted to determine the effect of vortex tube curvature on their performance. A three dimensional CFD model that utilizes the RNG k-ε turbulence model is employed for the numerical simulations. The flow and temperature field in curved vortex tubes with curvature angles are simulated in the range of 0° (straight) to 150°. The tangential (swirl), axial velocity components and flow patterns including secondary circulation flow are evaluated. The objective of this work is the demonstration of the successful use of CFD in this regard, thereby providing a powerful tool that can be used to optimize vortex tube design as well as assess its feasibility in the context of new applications. The results are then used for evaluating the coefficient of performance (COP) of the vortex tube as a cooling solution.**

***Keywords*: Counter flow vortex tube, Turbulence model, Swirl velocity, Temperature separation.**

1. Introduction

A vortex tube, invented by Ranque, is a simple and essentially compact device having capability to divide input stream of pressurized air into simultaneous streams of hot and cold air at reduced pressure. When pressurized air is admitted into the vortex tube in tangential direction, it attains high swirl velocity. This motion sets up a vortex type of flow inside the tube. Due to internal mechanism, one of the streams exiting the tube is at lesser, while other stream is at higher temperature than that of input air stream. This phenomenon is known as energy separation or temperature separation. By controlling the position of control valve located on the hot side of the tube, mass of cold and hot air coming out of vortex tube can be controlled. The magnitude of temperature separation is affected with change in mass of cold gas extracted i.e. cold mass fraction, the pressure of input stream and geometry of vortex tube.

The distinctive feature of vortex tube is that such temperature separation effect gets produced almost instantaneously, even without any moving parts or any chemical reaction inside the tube. Absence of moving parts enables vortex tube to have very low maintenance, thereby extended service life. Due to ability to produce instant cold and hot air, vortex tube finds use in important applications such as comfort suits of mine workers and spray painters, spot cooling of electronic components in limited space, gas liquefaction etc.

A. Phenomenological approach

This approach relies on observation and experimental data. It is specifically personalised to the geometrical shape of the vortex tube and the details of its flow and is designed to match the particular observables of the complex vortex tube flow, namely turbulence, acoustic phenomena, pressure fields, air velocities and many others. The earlier published models of the vortex tube are phenomenological.

They are:

1. Radial pressure difference: centrifugal compression and air expansion
2. Radial transfer of angular momentum
3. Radial acoustic streaming of energy
4. Radial heat pumping

More on these models can be found in recent review articles on vortex tubes.

The phenomenological models were developed at an earlier time when the turbine equation of Euler was not thoroughly analyzed; in the engineering literature, this equation is studied mostly to show the work output of a turbine; while temperature analysis is not performed since turbine cooling has more limited application unlike power generation, which is the main application of turbines. Phenomenological studies of the vortex tube in the past have been useful in presenting empirical data. However, due to the complexity of the vortex flow this empirical approach was able to show only aspects of the effect but was unable to explain its operating principle. Dedicated to empirical details, for a long time the empirical studies made the vortex tube effect appear enigmatic and its explanation a matter of debate.

B. Applications

Commercial vortex tubes are designed for industrial applications to produce a temperature drop of up to 71 °C

(127 °F). With no moving parts, no electricity, and no refrigerant, a vortex tube can produce refrigeration up to 6,000 BTU/h (1,800 W) using only filtered compressed air at 100 PSI (6.9 bar). A control valve in the hot air exhaust adjusts temperatures, flows and refrigeration over a wide range.

Vortex tubes are used for cooling of cutting tools (lathes and mills, both manually-operated and CNC machines) during machining. The vortex tube is well-matched to this application: machine shops generally already use compressed air, and a fast jet of cold air provides both cooling and removal of the "chips" produced by the tool.

2. Literature review

Balan, G. May, J. Schoberl, A stable high-order Spectral Difference method for hyperbolic conservation laws on triangular elements. a spectral difference (SD) method is developed for viscous flows on meshes with a mixture of triangular and quadrilateral elements. The standard SD method for triangular elements, which employs Lagrangian interpolating functions for fluxes, is not stable when the designed accuracy of spatial discretization is third order or higher. Unlike the standard SD method, the method examined here uses vector interpolating functions in the Raviart-Thomas (RT) spaces to construct continuous flux functions on reference elements. The spectral-difference Raviart-Thomas (SDRT) method was implemented on triangular-element meshes for inviscid flow only. Our present results demonstrated that the SDRT method is stable and high order accurate in 2 dimension (2D) for a number of test problems by using triangular, quadrilateral, and mixed-element meshes for both inviscid and viscous flows. A stability analysis is also performed for mixed elements. We found our current SDRT scheme is stable for 4th order accurate spatial discretization's. However, a stable 5th order SDRT scheme remains to be identified.

C. Liang, S. Premasuthan, A. Jameson, Z. Wang, Large eddy simulation of compressible turbulent channel flow with spectral difference method. Quadrilateral elements are favored for solving boundary-layer problems, but mixed-element meshes with both quadrilateral and triangular elements are sometimes more straightforward in unstructured-grid generation. Studies have been done for the standard SD method on mixed-element meshes. However, no test has been done on the SDRT method with 2D quadrilateral elements. Its performance remains to be verified and validated. For mixed element meshes, we use two sets of shape functions for triangles and quadrilaterals, respectively, in order to setup the SDRT method. The SDRT scheme on triangular elements was studied and good performance was demonstrated. In this study, we will extend the numerical experiments to include quadrilateral elements, and further test the performance of the SDRT method on mixed-element grids. In addition, studies on the SDRT method were performed only for inviscid flows so far. In this present study, we will extend the application of SDRT method to viscous flows.

M. Baghdad, A. Ouadha, O. Imine, Y. Addad, Numerical study of energy separation in a vortex tube with different RANS models, finite volume approach with standard k-ε model and an algebraic stress model (ASM) with (Upwind, Hybrid, SOU, and QUICK schemes) to carry out their computations. The results showed that ASM performs better agreement between the numerical results. RANS and LES techniques to simulate the turbulent flow in a Ranque-Hilsch vortex tube. RANS computations have been executed on an axis-symmetric tow-dimensional mesh and results have been compared with LES one. The results suggested that all the simulations confirmed that radial velocity values are very small when compared with axial and tangential ones. RANS and LES can simulate secondary circulation flow inside a RHVT. They employed an axisymmetric model and compared the effects of different Reynolds Averaged Navier-Stokes (RANS). They used the standard k-ε, RNG k-ε, standard k-ω and SST k-ω turbulence model for predicting the temperature separation in Ranque-Hilsch vortex tube. Interestingly, the results indicated a better agreement between the predictions of the standard k-ε model and the experimental data.

G. L. Ranque, Method and apparatus for obtaining from a fluid under pressure two currents of fluids at different temperatures, the vortex tube thermal separation phenomenon comes from diffusion process of mean kinetic energy causing high rotating speed motion in vortex tube. There are several parameters for increasing thermal separation phenomenon and diffusion process such as diameter, length, number and size of nozzles.

H. M. Skye, G. F. Nellis, S. A. Klein, Comparison of CFD analysis to empirical data in commercial vortex tube. represents the effect of axial curvature on the efficiency of vortex tubes for various cold mass fractions at inlet pressures P = 2 bar. The straight vortex tube has the highest efficiency among the vortex tubes, but the 90° curved vortex tube has the lowest efficiency among them. Curvature of main tube reduces efficiency of vortex tubes, the maximum efficiency takes place in the vicinity of yc = 0.3 for all vortex tubes. The performance characteristics of the vortex tubes have been appraised by calculating the coefficient of performance (COP). The effect of axial curvature on the coefficient of performance of vortex tubes for various cold mass fractions at inlet pressure of 2 bar. For 0 b yc b 0.6 all vortex tubes are approximately in the same COP values. Maximum COP value is for straight vortex tube and minimum is for 90° curved vortex tube. At yc ≈ 0.6, all curved vortex tubes have a maximum COP value and for straight is at 26.2.

Seyed Ehsan Rafiee, M.M. Sadeghiazad, Three-dimensional and experimental investigation on the effect of cone length of throttle valve on thermal performance of vortex-tube using k-epsilon turbulence model, single-circuit vortex tube. This kind of device, in the simplest case, is a tube of cylindrical or conical shape, which has a tangential nozzle inlet for compressed gas, often air. Compressed gas passing through this nozzle inlet is injected in the energy separation chamber and forms the vortex

flow in it. Therefore, cold and hot gas flows out from different sides of the vortex tube. If an additional inlet is added near the hot outlet, it is possible to increase hot and cold mass flow rates, while maintaining the same temperature difference. Such a kind of device is called double-circuit vortex tube. To the best of authors' knowledge, there are no available works in literature dealing with the numerical investigation of double- circuit vortex tubes. Thus, it is intention of the authors to bridge this gap by means of the present paper, which represents the first attempt to perform an extensive numerical investigation devoted to the study of a double-circuit vortex tube.

J. Lewins, A. Bejan, Vortex tube optimization theory, Inlet: Properties at the inlet are usually obtained from experimental data, analysis, or estimation. It is very rare that all the boundary conditions required are available from experiments. At inlet properties are usually obtained from experimental data. Compressed gas enters the vortex tube tangentially through two nozzles. Most experiments provide inlet data such as pressure Pin, temperature Tin and mass flow rate m· just before the nozzles. For this study, both compressed air with known pressure and total temperature at the inlet are assumed. Wall: Since the vortex tube was made of brass and covered with the insulator, then no slip and adiabatic conditions for tube walls are used.

S.U. Nimbalkar, M.R. Muller, An experimental investigation of the optimum geometry for the cold end orifice of a vortex tube,_ experimental and numerical studies are conducted to deter- mine the optimum values for vortex tube dimension such as length, diameter, and cold orifice. Curvature of vortex tube can be an important parameter in finding the optimum vortex tube corresponding to the highest efficiency. In this present study, a detailed analysis of various angle of curvature of the vortex tube has been carried out through CFD techniques to simulate the phenomenon of energy separation, temperature and velocity gradients.

K. Dincer, Experimental investigation of the effects of three fold type Ranque–Hilsch vortex tube and six cascade type Ranque–Hilsch vortex tube on the performance of counter flow Ranque–Hilsch vortex tubes, the energy separation phenomenon inside the vortex tube. Due investigated the progress of exploring the structure inside the vortex tube. Dincer experimentally investigated three different situations; conventional RHVT, threefold cascade type RHVT and six cascade type RHVT, respectively. The results show that maximum values of temperature difference and cold mass fraction are 67.6 °C and 0.9 for the last situation. Energy separation performance of vortex tube can be improved by using divergent tube. Xue and Arjomandi investigated the effect of the vortex angle on the performance of the Ranque–Hilsch vortex tube. They discovered that vortex angle played an important role in vortex tube performance. Also their results show that a smaller vortex angle creates a larger temperature difference and has better performance. They also stated that inlet pressure of 4 bar makes the highest efficiency. A critical review of a temperature separation in a vortex tube has been done by Xue et. al. Hypotheses of pressure, viscosity, turbulence, temperature, secondary circulation and acoustic streaming are discussed in their work.

U. Behera, P.J. Paul, S. Kasthurirengan, R. Karunanithi, S.N. Ram, K. Dinesh, S. Jacob, CFD analysis and experimental investigations towards optimizing the parameters of Ranque–Hilsch vortex tube, the flow in the tube is split into two helical co-axial streams with different thermal features. For all profile of vortex tubes, flow near the wall is hot, and near the axis is cold. All vortex tubes yield an internal recirculation zone near the inlet with different sizes of recirculation in each case. At the exit of nozzle inlets, some vortices are produced which increases the number and size as the curvature values increase. Results show that vortices play a major role in mixing inner and peripheral flows inside the vortex tube. The gas leaving the inlet nozzle at high velocity creates a rapidly spinning vortex in the tube. There is large energy transfer from the inner and peripheral region that is related to viscous shear in the tangential direction. Curved vortex tube gets negative values of tangential velocity in some upper region of vortex tube which means that the energy transfers decreases.

3. Vortex tube refrigeration

It is one of the non-conventional type refrigerating systems for the production of refrigeration. The schematic diagram of vortex tube is shown in the fig. 1.

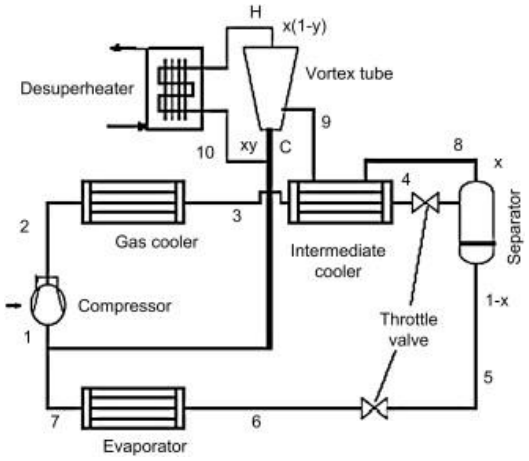

Fig. 1. Cycle parameter optimization of vortex tube refrigeration

It consists of nozzle, diaphragm, valve, hot-air side, cold-air side. The nozzles are of converging or diverging or converging-diverging type as per the design. An efficient nozzle is designed to have higher velocity, greater mass flow and minimum inlet losses. Chamber is a portion of nozzle that facilities the tangential entry of high velocity airstream into hot side. Generally, the chambers are not of circular form, but they are gradually converted into spiral form. Hot side is cylindrical in cross section and is of different lengths as per design. Valve obstructs the flow of air through hot side and it also controls the

quantity of hot air through vortex tube. Diaphragm is a cylindrical piece of small thickness and having a small hole of specific diameter at the center. Air stream traveling through the core of the hot side is emitted through the diaphragm hole. Cold side is a cylindrical portion through which cold air is passed.

A. Working principle of vortex tube refrigeration

Compressed air is passed through the nozzle as shown in fig 3.2. Here, air expands and acquires high velocity due to particular shape of the nozzle. A vortex flow is created in the chamber and air travels in spiral like motion along the periphery of the hot side. This flow is restricted by the valve. When the pressure of the air near valve is made more than outside by partly closing the valve, a reversed axial flow through the core of the hot side starts from high-pressure region to low pressure region. During this process, heat transfer takes place between reversed and forward stream.

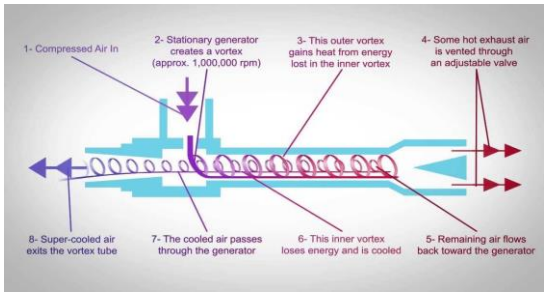

Fig. 2. Working of vortex tube refrigeration

Therefore, air stream through the core gets cooled below the inlet temperature of the air in the vortex tube, while air stream in forward direction gets heated up. The cold stream is escaped through the diaphragm hole into the cold side, while hot stream is passed through the opening of the valve. By controlling the opening of the valve, the quantity of the cold air and its temperature can be varied.

4. Modeling of vortex tube

A. Mathematical modeling

The governing equations solved by Fluent 6.3.26 are equation of continuity, momentum, energy and equation of state, given below.

$$\frac{\partial \rho}{\partial t} + \nabla . \rho \vec{v} = S_m \quad (1)$$

$$\frac{\partial}{\partial t}(\rho \vec{v}) + \nabla . (\rho \vec{v}\vec{v}) = -\nabla p + \nabla . (\bar{\bar{\tau}}) + \rho \vec{g} + \vec{F}, \quad (2)$$

$$\frac{\partial \rho h_o}{\partial t} - \frac{\partial P}{\partial t} + \mathrm{div}(\rho h_o \mathrm{U}) = \mathrm{div}\ \lambda\, \mathrm{grad}\, T_s \quad (3)$$

$$P = \rho R T_s \quad (4)$$

Transport equations in Standard k-ε model are for turbulence kinetic energy, *k*, and its rate of dissipation, ε, given below,

$$\frac{\partial}{\partial t}(\rho k) + \frac{\partial}{\partial x_i}(\rho k u_i) = \frac{\partial}{\partial x_j}\left[\left(\mu + \frac{\mu_t}{\sigma_k}\right)\frac{\partial k}{\partial x_j}\right] + G_k + G_b - \rho\varepsilon - Y_M + S_k \quad (5)$$

$$\frac{\partial}{\partial t}(\rho \varepsilon) + \frac{\partial}{\partial x_i}(\rho \varepsilon u_i) = \frac{\partial}{\partial x_j}\left[\left(\mu + \frac{\mu_t}{\sigma_\varepsilon}\right)\frac{\partial \varepsilon}{\partial x_j}\right] + C_{1\varepsilon}\frac{\varepsilon}{k}\left(G_k + C_{3\varepsilon}G_b\right) - C_{2\varepsilon}\rho\frac{\varepsilon^2}{k} + S_\varepsilon \quad (6)$$

B. Boundary conditions

For present CFD study, geometry of vortex tube as well as boundary conditions of experimental study has been used. Details about this have been avoided here for the sake of brevity and can be found in the work. The structured grid has been created using Gambit while mathematical equations have been solved using commercially available code Fluent 6.3.26. The meshed vortex tube is depicted in Fig. 3.

All the CFD simulations have been performed in steady state mode using pressure based implicit solver. The standard k–ε model has been used to model the turbulent flow inside the tube. The flow inside the vortex tube is compressible. The inlet of vortex tube is considered as mass flow inlet. The hot end and cold end are considered as pressure outlet. The cold end is open to atmosphere. Gravity is neglected. Pressure on hot end is varied to obtain various cold mass fractions. SIMPLE algorithm is used for Pressure-Velocity Coupling. Default values of Under Relaxation Factors have been used. To set the convergence criteria, default values of residuals of the order of 10^{-6} were used for energy while it was 10^{-3} for all other quantities. Wall of the vortex tube is assumed to be stationary and adiabatic with no-slip boundary condition.

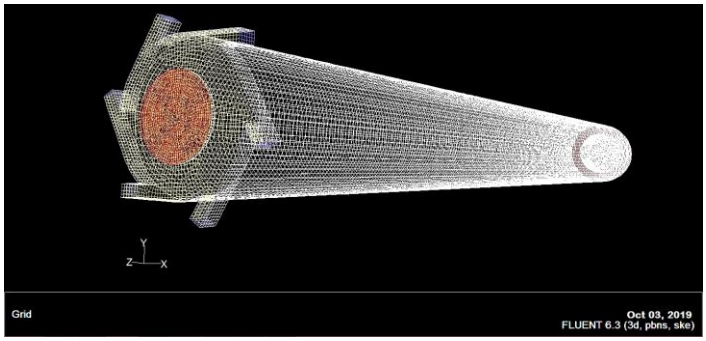

Fig. 3. Structured mesh of vortex tube used in present simulation

5. Validation

A. Grid independence study

Grid independence of solution has been checked using structured grid of different sizes i.e. with 32215, 98510 and 152553 cells. This check is necessary so as to eliminate the errors arising due to coarseness of the grid. This is shown in Fig. 4.

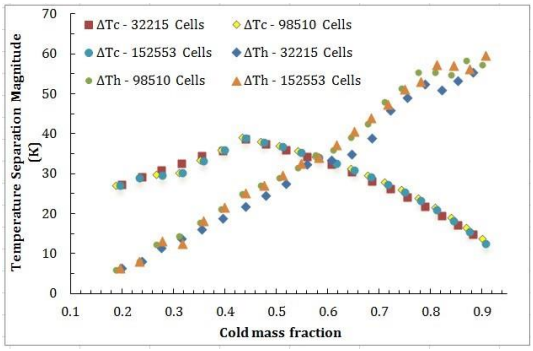

Fig. 4. Effect of grid size on temperature separation magnitude

As observed from Fig. 4, for all the grid sizes, magnitude of temperature separation is nearly same at all values of cold mass fractions. Hence, further study has been carried out for grid size of 152553 cells.

Results of present CFD study are compared with experimental and CFD results of Skye for validation and authentication. As observed from Fig. 4, results of present CFD study are in good agreement with experimental results. It implies that simulation methodology followed in present work is appropriate.

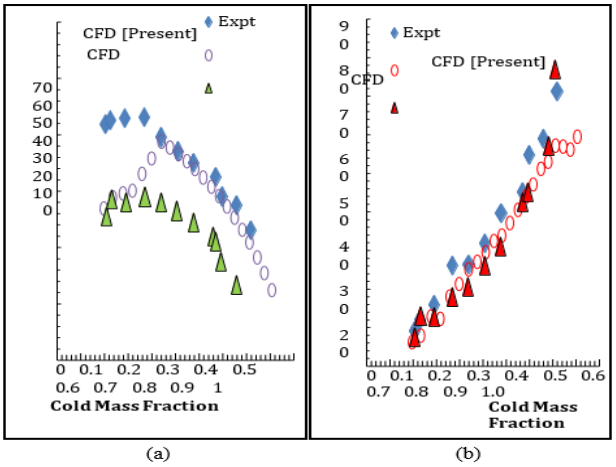

Fig. 5. Comparison of CFD results (a) Cold End (b) Hot End Temperature Separation

B. *Velocity and pressure pattern at nozzle section*

Fluid with high pressure enters into the vortex tube. Pressure in the inlet is the source of energy. Most pressure drop takes place within the nozzle whereas velocity increases very sharply and a circular flow is established. Fig. 5(a),(b) shows the visualization of the pressure and velocity fields at inlet section of the curved vortex tube. Pressure drops down to 2.2 kPa from 3 kPa at inlet while the velocity increases very sharply about 450 m/s. Because the ideal gas was assumed, the density distribution is similar to pressure in vortex tube.

C. *Velocity and pressure distribution*

With the experimental methods, determination of the velocity distributions in vortex tube is impossible. However, by using the CFD model, we can clarify the velocity components in all regions of vortex tube. The radial profiles of velocity components in swirl, axial and radial are shown respective for straight vortex tube, 90° and 110° curved vortex tubes at different cross section locations of S = 10, 70 and 140 mm. In every cross sections, the swirl velocity is predominant velocity component. The magnitude of the swirl velocity decreases towards the hot end exit. The radial profile of the swirl velocity indicates a free vortex near the wall and the values become negligibly small at the core.

The results for straight vortex tube are in conformity with the observations of Behara, Korosaka and Gutsol. The fluid at the core of the vortex tube has very low kinetic energy due to the minimum swirl fluid velocity at the central zone of the tube. The maximum value of swirl velocity of about 450 m/s occurs at the inlet zone. In the curved vortex tubes, the tangential velocity profile is not symmetric, which is mainly caused by the centrifugal effect generated by the curvature of the tube.

D. *Temperature distribution and secondary flow circulation*

Radial profiles of the total temperature at different cross section lo- cations (S = 10, 70 and 140 mm) for θ = 0 (straight vortex tube), 90° and 150° curved vortex tubes are presented in Fig. 6. Maximum total temperature is near the periphery of the tube wall. In all section the straight tube has maximum total temperature. Minimum total temperature was observed near exit center of tube. Also the straight profile has minimum total temperature.

The results show that maximum and minimum total temperature gradients are for straight vortex tube and 90° curved vortex tube. The temperature gradient for 150° curved vortex tube is higher than 90° curved vortex tube. So energy separation in 150° curved vortex tube is higher than 90° curved vortex tube. Maximum energy separation is for straight profile. The total temperatures with stream trace are plotted as contour plot for straight vortex tube, 30° and 60° curved vortex tubes, respectively.

For cold mass fraction about 0.5, giving maximum hot gas temperatures of 313, 315.3, and 314.9 K and minimum cold gas temperatures of 281, 285.6, and 286.8 K for straight, 30° and 60° curved vortex tubes, respectively. To verify the existence of secondary circulation flow in vortex tube and its influence on temperature separation, in table 1 the stream trace is plotted. It shows that inside the straight vortex tube there exist two swirling flows.

One flow swirls to the hot end in the peripheral region, named the peripheral swirling flow. The other flow anti-swirls to the cold exit in the center region, named the internal swirling flow. Those swirl flows generate the high rotating speed vortex motion inside the vortex tube, Table 1 shows it obviously for straight, 30°, 60°, 90°, 110° and 150° curved vortex tubes.

There are also two loops for straight vortex tube, named the secondary circulation (SC) loop. This loop acts as the high and low temperature environments like in a normal refrigeration cycle. Internal energy is transferred between the inner and peripheral regions via the two loops. The incoming gas element and the gas element in the loop mix together. Some gas elements in this loop first pass the peripheral region from the entrance to the hot end, and escape from the hot end. Other gas elements stay in the loop and return axial direction to the cold end in the center, and exit via the cold exhaust. For 30° curved vortex tube, stream trace is shown in Fig. 5(b). Temperature distribution shows that vortices play a major role in energy separation.

In fact, vortices in SC-loop cause mixing of center inner cold flow with peripheral hot flow. Increase of the number of vortices causes more mixing. The 30° curved vortex tube has five vortices, thus it has lower refrigerating capacity than

straight. Also for 60° curved vortex tube, it has 9 vortices and so it has lower cooling performance than 30° curved vortex tube and straight vortex tube.

Table 1 presents the minimum temperature, number of vertices and length of the SC-loop where SC-loop is the distance from cold exit to the end of secondary circulation loop (the point that axial velocity is zero) for P = 3 bar and y_c = 0.5. The number of vortices for 60°, 90°, 110° and 150° curved vortex tubes is nine but the length of SC-loop is different, thus this parameter has an important role in cooling performance of these profiles. Because by increasing the length of SC-loop, gas elements stay in the loop and moves longer distance and losses (earns) more energy. In fact, the number of vortices is fixed but growing and it causes the gas elements in the loop pass more distance and loss more energy.

Minimum temperature, number of vortices and length of the SC-loop for different vortex tubes profile at P = 3 bar and y_c = 0.5.

Table 1
Stream trace for the inner core fluid flow and peripheral hot fluid flow in the entire straight, 30°, 60°, 90°, 110° and 150° curved vortex tubes in three-dimensional space

Vortex tube profiles	Minimum temperature (K)	Number of vertices	Length of SC-Loop (mm)
θ = 0°	280.2	2	287
θ = 30°	285.6	5	320
θ = 60°	286.8	9	330
θ = 90°	288.4	9	340
θ = 110°	284.3	9	350
θ = 150°	282.2	9	360

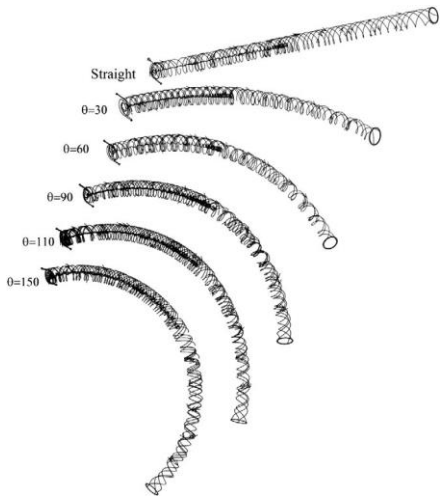

Fig. 6. Various θ = 0°, 30°, 60°, 90°, 110°, 150°, curved vortex tubes in three-dimensional space

E. Thermal analysis of vortex tube refrigerator

CFD studies were carried out to verify the existence of secondary circulation flow in vortex tube and its influence on temperature separation for different curvature angle values and also find the optimized curved vortex tube. Fig. 7, shows the cold temperature difference versus the cold mass fraction at P = 2 bar. The maximum cold temperature difference is about 15.1 K for straight at y_c = 0.28. Lowest cold temperature difference is 2.89 k for 90° curvatures at y_c = 0.91. It is obvious that cold temperature difference is increased by increasing in the cold mass fraction about 0.3. For 0.6 = y_c = 1, all vortex tubes are approximately in the same cold temperature difference.

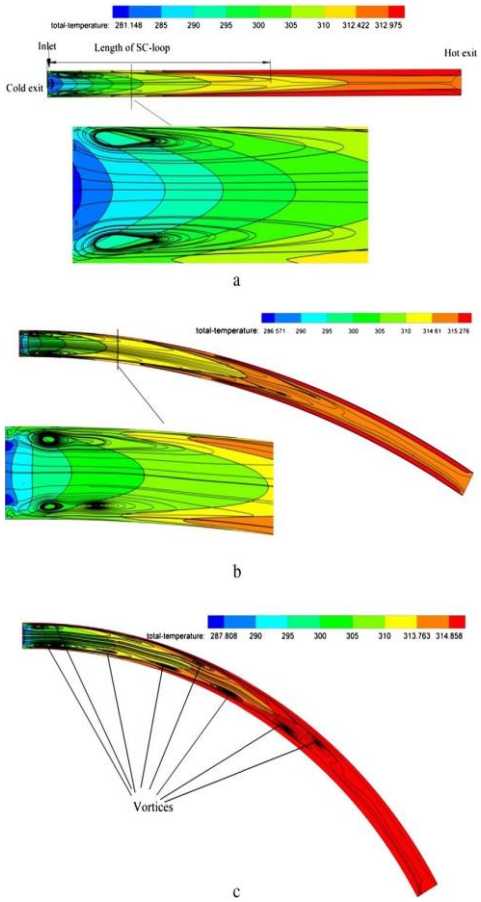

Fig. 7. Total temperature maps with streamline patterns superimposed for (a) straight, (b) 30° curved and (c) 60° curved vortex tube for P = 2 bar

Fig. 7(a) represents the effect of axial curvature on the efficiency of vortex tubes for various cold mass fractions at inlet pressures P = 2 bar. The straight vortex tube has the highest efficiency among the vortex tubes, but the 90° curved vortex tube has the lowest efficiency among them. Curvature of main tube reduces efficiency of vortex tubes, the maximum efficiency takes place in the vicinity of y_c = 0.3 for all vortex tubes.

The performance characteristics of the vortex tubes have been appraised by calculating the coefficient of performance (COP). Fig. 7(c), represents the effect of axial curvature on the coefficient of performance of vortex tubes for various cold mass fractions at inlet pressure of 2 bar. For 0≈ y_c ≈ 0.6 all vortex tubes are approximately in the same COP values. Maximum COP value is for straight vortex tube and minimum is for 90° curved vortex tube. At y_c ≈ 0.6, all curved vortex tubes have a maximum COP value and for straight is at 26.2. Fig. 7 is for

investigate the effect of radius of curvature on COP of vortex tube at constant cold mass fractions 0.3 and 0.5. The models with different R/D ratios i.e. (straight), 40.1, 20.05, 13.36, 10.94, and the 8.02 with 400 mm length and D = 19.05 mm, have been studied. As it is clear, for inlet pressure P = 3 bar minimum COP points occur for R/D = 13.36 (90° curved vortex tube). By increasing R/D from 0 to 13.36 the COP decreased, and in region R/D N 13.36 the COP increased.

6. Result and discussion

This section presents nature of flow parameters inside vortex tube. Fig. 8, illustrates contours of swirl velocity inside vortex tube. Swirl velocity is maximum at nozzle inlet. It is found to decrease with an increase in axial distance i.e. as flow of air progresses towards hot end. Swirl velocity is minimum near the hot end. Along the radial direction of the tube, the swirl velocity is observed to have the minimum magnitude near the tube axis. Throughout the tube, inner core is observed to have negligible swirl velocity.

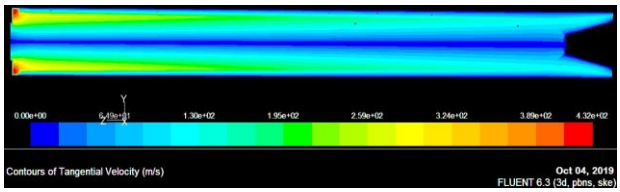

Fig. 8. Contours of tangential or swirl velocity inside vortex tube

Fig. 8, shows variation of swirl velocity at different axial locations. At all axial locations swirl velocity increases with radius i.e. towards the periphery. Near the wall of the tube, swirl velocity suddenly drops down to zero due to no-slip boundary condition at the wall. Magnitude of swirl velocity decreases with increase in axial distance from cold end.

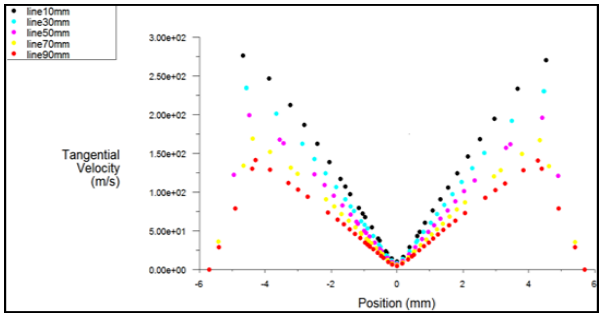

Fig. 9. Swirl velocity at different axial locations

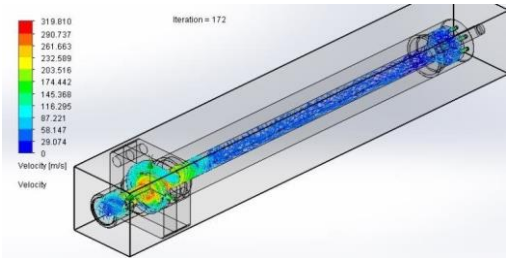

Fig. 10. Various velocities inside the vortex tube

Fig. 11, shows variation of axial velocity inside vortex tube. It is observed that the maximum axial velocity in hot region is near the tube wall and the direction of the flow near the wall is towards the hot end exit. The direction of the flow along the axis is towards the cold end exit. Also, the maximum value of the axial velocity in hot region decreased with increasing axial distance. The axial velocity in the cold core was found to increase with a decrease in the axial distance i.e. as we move from hot exit to cold exit.

The drag force caused by the difference of pressure between flow field and cold end exit will continuously act on particles moving towards the hot end. When the particle is not left with any momentum to flow against this pressure gradient, its axial velocity ceases to zero and later on reverse its direction of flow, by moving towards the cold end exit. Further acted by the differential pressure, the particle expands causing to considerable increase in axial velocity in reverse direction.

Fig. 15, shows streamline structure inside vortex tube. First, the air introduced in the vortex tube via the inlets positioned at a given angle of the main pipe, creates vortices in the internal flow. The model selected is capable of predicting this flow behavior which is expected as this is imposed mainly by the angular position of the inlet sections. In addition, the figure illustrates the existence of two vortices, both; rotating in the same direction with the same angular velocity. This is consistent with observation of Baghdad, shown in Fig. 16.

The first is a free vortex that characterizes the outer regions and tends to escape through the hot exit, whereas the second one is a forced vortex representing the reverse flow that appears in the core region and moves back towards the cold exit crossing all the hot tube and the vortex chamber Centre. It can also be noticed that the reverse flow starts moving towards the cold exit at a specific location along the main tube.

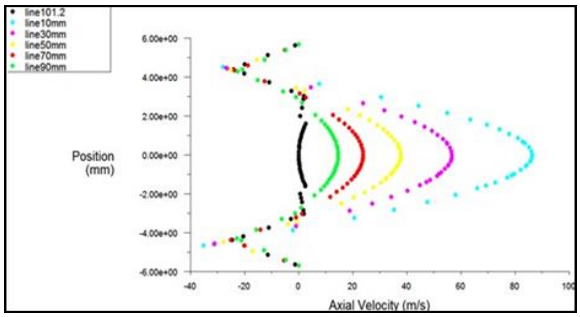

Fig. 11. Variation of axial velocity inside vortex tube

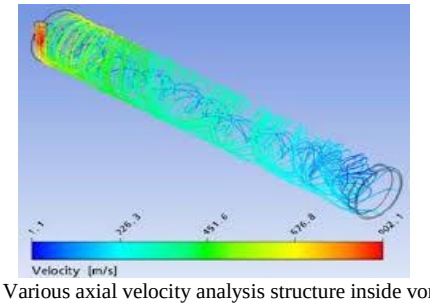

Fig. 12. Various axial velocity analysis structure inside vortex tube

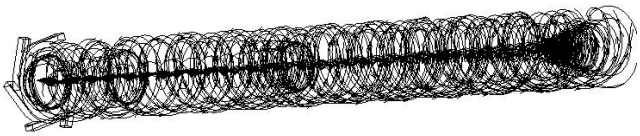

Fig. 13. Streamline structure inside vortex tube [Present]

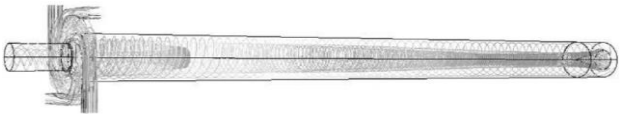

Fig. 14. Streamline structure inside vortex tube

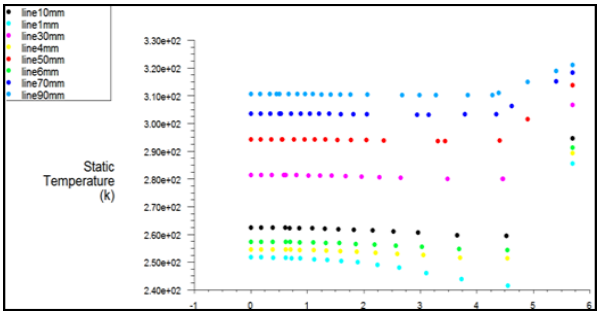

Fig. 15. Static temperature inside vortex tube

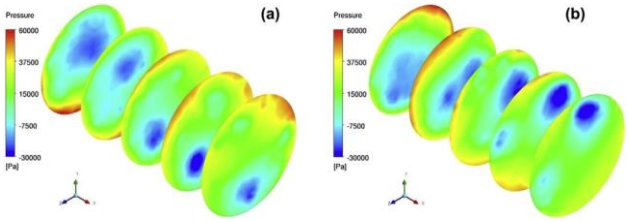

Fig. 16. Static pressure contour plots in the cross sections of the vortex tube predicted using LES n.14 at different time: (a) t ¼ 0.011 s; (b) t ¼ 0.016 s

Fig. 17. illustrates the static temperature as a function of radius at different axial locations and shows that the static temperature decreases in the radial direction (as r gets larger), except very near the tube inlet. The decrease in static temperature in radial direction creates the temperature gradient for the heat energy to flow radially. This temperature gradient is maintained throughout the vortex tube length by the velocity gradient in radial direction. Due to no slip boundary condition at the wall, static temperature increases very near to wall because of conversion of kinetic energy into thermal energy. In this region heat transfer will be in negative radial direction i.e. radially inwards.

Fig. 18, shows magnitude of total temperature inside vortex tube at different axial locations. Total temperature increases with increase in axial distance. The total temperature profiles depend upon distribution of kinetic energy in vortex tube. Comparing the total temperature and the swirl velocity profiles, we observe that the low temperature zone in the core coincides with the negligible swirl velocity zone.

Fig. 19, shows contours of total temperature inside vortex tube observed during our study. The phenomenon of temperature separation is clearly visible in this contour plot. The peripheral flow is warm and core axial flow is cold relative to the inlet flow. Maximum total temperature is observed near hot end of tube. Magnitude of temperature separation decreases with increase in axial distance.

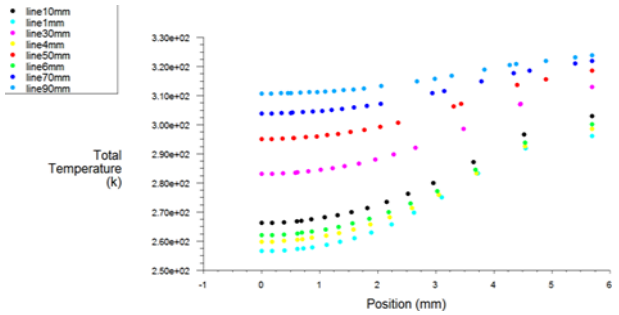

Fig. 17. Total temperature inside vortex tube

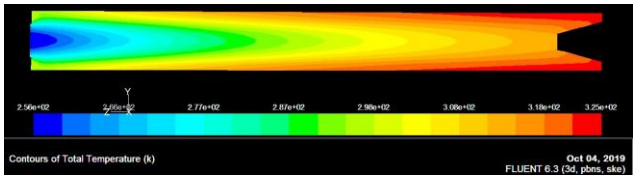

Fig. 18. Contours of total temperature inside vortex tube

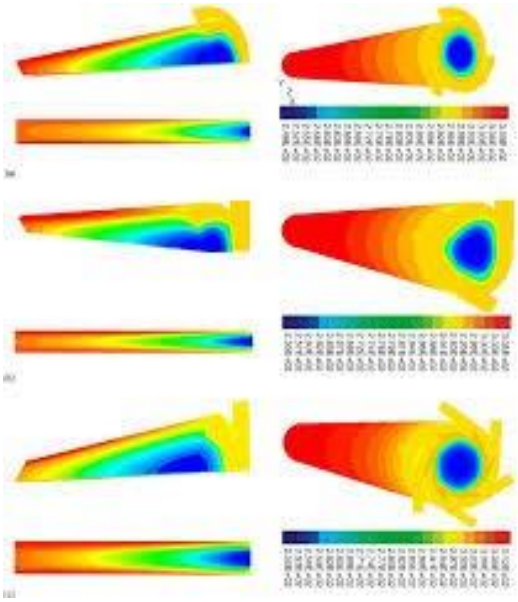

Fig. 19. Temperature distribution over the tubes

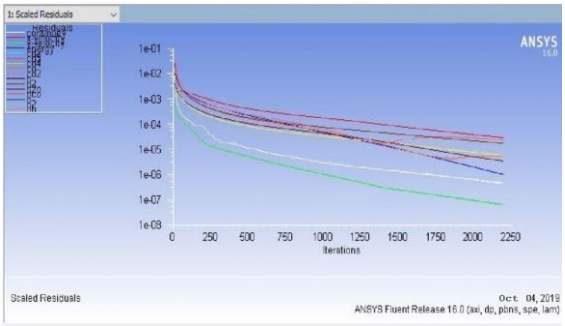

Fig. 20. Convergence residual of vortex tube

7. Conclusion

CFD simulation of vortex tube was attempted in order to understand nature of flow physics inside the tube. It is concluded that CFD results are in good agreement with experimental results. Swirl velocity is the largest component of flow velocity. Profile of axial velocity clearly indicates presence of flow reversal inside the tube. Core axial flow is colder while peripheral flow is hotter than inlet air. Static temperature decreases towards periphery which can cause heat transfer from core axial to peripheral air mass.

The gas leaving the inlet nozzle at high velocity creates a rapidly spinning vortex in the tube. There is large energy transfer from the inner and peripheral region that is related to viscous shear in the tangential direction. Curved vortex tube gets negative values of tangential velocity in some upper region of vortex tube which means that the energy transfers decreases.

Curvature of vortex tube causes decrease in the swirl velocity and the diffusion process in vortex tube. Results show that the straight and 150° curved vortex tube have higher performance as a refrigerator than other curvature angles.

The analysis shows that the vortex tube thermal separation phenomenon comes from diffusion process of mean kinetic energy causing high rotating speed motion in vortex tube. There are several parameters for increasing thermal separation phenomenon and diffusion process such as diameter, length, number and size of nozzles.

Results show that the flow in the tube is split into two helical co-axial streams with different thermal features. For all profile of vortex tubes, flow near the wall is hot, and near the axis is cold. All vortex tubes yield an internal recirculation zone near the inlet with different sizes of recirculation in each case. At the exit of nozzle inlets, some vortices are produced which increases the number and size as the curvature values increase. Results show that vortices play a major role in mixing inner and peripheral flows inside the vortex tube.

References

[1] G. L. Ranque, Method and apparatus for obtaining from a fuid under pressure two currents of fluids at different temperatures, U.S. Patent No. 1952281, 1934.
[2] B. Ahlborn, S. Groves, Secondary Flow in Vortex Tube, Fluid Dynamic Research, 21 (1997) 73–86.
[3] R. Shamsoddini, A. H. Nezhad, “Numerical analysis of the effects of nozzles number on the flow and power of cooling of a vortex tube,” Int. J. Refrigeration. vol. 33 pp. 774–782, 2010.
[4] T. T. Cockerill, “Fluid mechanics and thermodynamics of a Ranque-Hilsch vortex tube,” Master Thesis, University of Cambridge, 1995.
[5] T. Dutta, K.P. Sinhamahapatra, S. S. Bandyopdhyay, “Comparison of different turbulence models in predicting the temperature separation in a Ranque Hilsch vortex tube,” Int. J. Refrigeration. vol. 33 pp. 783–792, 2010.
[6] M. Baghdad A. Ouadha, O. Imine, Y. Addad, “Numerical study of energy separation in a vortex tube with different RANS models,” Int. J. The. Sci. vol. 50 pp. 2377-2385, 2011.
[7] H. M. Skye, G. F. Nellis, S. A. Klein, “Comparison of CFD analysis to empirical data in commercial vortex tube,” Int. J. Refrig. vol. 29 pp. 71–80, 2006.
[8] M. Baghdad, A. Ouadha, O. Imine, Y. Addad, “Numerical study of energy separation in a vortex tube with different RANS models,” Int. J. Therm. Sci. 50, 2011, 2377-2385.
[9] S.U. Nimbalkar, M.R. Muller, “An experimental investigation of the optimum geometry for the cold end orifice of a vortex tube,” Appl. Therm. Eng. 29, 2009, 509-514.
[10] O. Aydin, B. Markal, M. Avci, A new vortex generator geometry for a counter flow Ranque-Hilsch vortex tube, Appl. Therm. Eng. 30, 2010, 2505-2511.
[11] Seyed Ehsan Rafiee, M.M. Sadeghiazad, “Three-dimensional and experimental investigation on the effect of cone length of throttle valve on thermal performance of a vortex tube using kee turbulence model,” Appl. Therm. Eng. 66, 2014, 65-74.
[12] Masoud Bovand, Mohammad Sadegh Valipour, Smith Eiamsaard, Ali Tamayol, “Numerical analysis for curved vortex tube optimization,” Int. Commun. Heat Mass Transfer, 50, 2014, 98-107.
[13] Mohammad Sadegh Valipour, Nima Niazi, Experimental modeling of a curved RanqueeHilsch vortex tube refrigerator,” Int. J. Refrig. 34, 2011, 1109-1116.
[14] H.M. Skye, G.F. Nellis, S.A. Klein, “Comparison of CFD analysis to empirical data in a commercial vortex tube,” Int. J. Refrig. 29, 2006, 71-80.
[15] H. Pouraria, M.R. Zangooee, Numerical investigation of vortex tube refrigerator with a divergent hot tube, Energy Procedia. 14, 2012, 1554-1559.
[16] S. Eiamsa-Ard, P. Promvonge, “Review of Ranquee Hilsch effects in vortex tubes,” Renew. Sustain. Energy Rev. 12, 2008, 1822-1842.
[17] S. A. Piralishvili, V. M. Polyaev, “Flow and thermodynamic characteristics of energy separation in a double-circuit vortex tube an experimental investigation,” Exp. Therm. Fluid Sci. 12, 1996, 399-410.
[18] A.P. Merkulov, Vikhrevoi Effekt I. Ego Primenenie V. Tekhnike “Vortex Effect and its Application in Technique, in Mechanical Engineering, Mashinostroenie, Moscow, 1969.
[19] J. H. Ferziger, M. Peric, “Computational Methods for Fluid Dynamics,” Springer, Heidelberg, 2002.
[20] C. A. J. Fletcher, “Computational Techniques for Fluid Dynamics,” Springer, Heidelberg, 1991.